THE ASTROPHYSICAL JOURNAL, 551:478–485, 2001 April 10

BORON IN PRESOLAR SILICON CARBIDE GRAINS FROM SUPERNOVAE

P. HOPPE,[1] K. LODDERS,[2] R. STREBEL,[1] S. AMARI,[3] AND R. S. LEWIS[4]

Received 2000 August 11; accepted 2000 December 3

ABSTRACT

Eleven presolar silicon carbide grains of type X separated from the Murchison meteorite have been analyzed for boron abundances and isotopic compositions by secondary ion mass spectrometry. Boron concentrations are low with typical B/Si ratios of $\approx 1 \times 10^{-5}$. The average $^{11}B/^{10}B$ ratio of 3.46 ± 1.39 is compatible with the solar system value but might be affected by contaminating boron of laboratory origin. These data are compared with theoretical predictions for Type II supernovae, the most likely parent stars of X grains. The B/Si ratios of X grains are much lower (more than an order of magnitude on average) than expected from Type II supernova shell-mixing of matter from the C- and Si-rich zones, contrary to other elemental ratios such as Al/Si and Ti/Si. Condensation calculations show that with $C/O > 1$ in the ejecta, boron and aluminum will readily condense as BN and AlN, respectively, into silicon carbide, and the B/Al ratio is expected to remain constant. The nitrogen, aluminum, and titanium abundances in SiC X grains are well reproduced by the condensation calculations. Given the similarity of the boron and aluminum condensation chemistry and the generally expected high B/Al ratios (relative to solar) in Type II supernova mixtures with $C/O > 1$, the observed difference between measured and predicted B/Al ratios must be considered a serious problem. Possible solutions include (1) lower than predicted boron production from Type II supernovae, (2) complex mixing scenarios in supernova ejecta involving only sublayers of the C-rich zones, and (3) formation of silicon carbide under conditions with $C/O < 0.1$.

Subject headings: circumstellar matter — dust, extinction — nuclear reactions, nucleosynthesis, abundances — supernovae: general

1. INTRODUCTION

Boron is bypassed by standard stellar nucleosynthesis. Its production relies mostly on spallation reactions between high-energy (>100 MeV) Galactic cosmic rays (GCR) and abundant target nuclei such as ^{12}C, ^{14}N, and ^{16}O in the interstellar medium (ISM). Standard GCR models predict $^{11}B/^{10}B$ ratios of ≈ 2.5 (e.g., Meneguzzi, Audouze, & Reeves 1971), which is distinctly lower than the solar system value of 4.04. The disagreement between the solar $^{11}B/^{10}B$ ratio and the predictions from standard GCR models has remained an unsolved puzzle. Two possible solutions have been proposed to overcome this problem.

The first solution is based on spallation reactions between low-energy (10–30 MeV) carbon and oxygen nuclei and interstellar hydrogen in star-forming regions. In addition to the light elements, several short-lived isotopes can be produced in such environments (Clayton 1994). The $^{11}B/^{10}B$ ratios are expected to be higher than solar (Meneguzzi et al. 1971; Cassé, Lehoucq, & Vangioni-Flam 1995), and it was argued that the solar system boron is a mixture of standard and low-energy GCR-produced boron (Cassé et al. 1995; Chaussidon & Robert 1995; Ramaty, Kozlovsky, & Lingenfelter 1996). The observation of gamma-ray lines at 4.4 and 6.1 MeV in the Orion star-forming region by COMPTEL (Bloemen et al. 1994) has been widely used as evidence for environments of extensive low-energy spallation reactions. However, this observational evidence has now turned out to be a spurious result (Bloemen et al. 1999), and convincing observational support for the existence of environments with extensive low-energy spallation reactions is still missing.

The second proposed solution is based on production of sufficient ^{11}B in Type II supernovae (SNe). Here ^{11}B is predicted to be produced from neutrino interactions with carbon in C-rich layers by the reactions $^{12}C(\nu, \nu'n)^{11}C(\beta^+\nu)^{11}B$ and $^{12}C(\nu, \nu'p)^{11}B$ and, to a lesser extent, by α-captures on ^{7}Li and ^{7}Be in the He layer (Woosley & Weaver 1995, hereafter WW95; Yoshida, Emori, & Nakazawa 2000). In the SN models of WW95, ^{11}B is heavily enriched in the ejecta (compared to its initial abundance at stellar birth) regardless of mass and metallicity of the progenitor stars. Galactic chemical evolution models that include SNe as a source of ^{11}B can well reproduce the solar boron abundance (Timmes, Woosley, & Weaver 1995) and solar $^{11}B/^{10}B$ ratio (Olive et al. 1994).

From an observational point of view the boron production in SNe might be pursued by the study of presolar dust grains found in primitive meteorites (Anders & Zinner 1993; Ott 1993; Zinner 1998; Hoppe & Zinner 2000). An important constituent of presolar dust is silicon carbide (SiC). These grains show large isotopic anomalies in the major elements carbon and silicon and many trace elements, pointing to carbon stars (most grains), novae, and SNe as stellar sources. The SiC particles from SNe are the so-called X grains. Compared to solar ratios, these grains have, mostly, higher $^{12}C/^{13}C$ (to 7000), lower $^{14}N/^{15}N$ (to

[1] Max-Planck-Institut für Chemie, Abteilung Kosmochemie, P.O. Box 3060, D-55020 Mainz, Germany; hoppe@mpch-mainz.mpg.de.
[2] Planetary Chemistry Laboratory, Department of Earth and Planetary Sciences, Washington University, St. Louis, MO 63130-4899; lodders@levee.wustl.edu.
[3] Laboratory for Space Sciences and the Physics Department, Washington University, St. Louis, MO 63130-4899; sa@howdy.wustl.edu.
[4] Enrico Fermi Institute, University of Chicago, 5630 Ellis Avenue, Chicago, IL 60637; r-lewis@uchicago.edu.

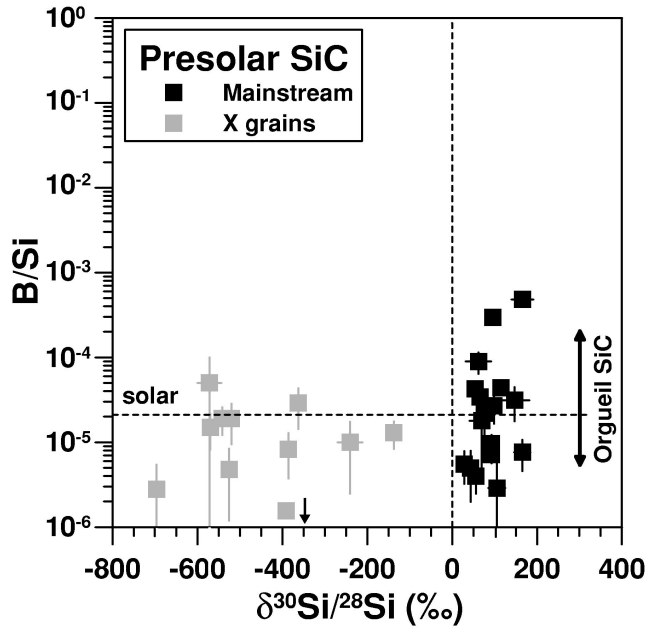

FIG. 1—B/Si and $^{30}Si/^{28}Si$ (as permil deviation from solar) ratios for presolar SiC X and mainstream grains from the Murchison CM2 meteorite. Errors are 1 σ. The dashed lines represent the solar values. The range of B/Si ratios observed in six SiC grains (four mainstream grains and one of type Y and one of type Z; for the classification of SiC grains, see Hoppe & Ott 1997) from the Orgueil CI meteorite (Huss et al. 1997) is shown for comparison.

13), and lower $^{29,30}Si/^{28}Si$ ratios (^{28}Si enriched up to a factor of 5). They also have high abundances of radiogenic ^{26}Mg and ^{44}Ca from the decay of radioactive ^{26}Al and ^{44}Ti (Amari et al. 1992; Nittler et al. 1995, 1996; Hoppe et al. 1996, 2000). These X grain isotopic signatures are distinct from those of the majority of SiC grains ("mainstream grains") and identified the X grains as SN condensates. They are thus ideal objects to study SN nucleosynthesis. We have measured the isotopic compositions and abundances of boron in 11 presolar silicon carbide grains of type X, about 1 μm in size, separated from the Murchison meteorite. We compare these boron isotopic and abundance data with expectations for condensation of boron into SiC in SN ejecta.

Our discussion focuses on Type II SNe as sources of SiC X grains. In order to verify the validity of the condensation calculations for boron, we also include N, Mg, Al, Ca, Ti, and Fe in the discussion, and the predictions for the elemental abundances are compared with those measured in ≈ 1 μm sized SiC X grains (Hoppe et al. 2000). Trace element abundances in SiC grains are determined by the composition of the source gas in the SN ejecta and the condensation behavior of the elements. The SN mixtures studied here are based on the mixing of isotopically homogenized discrete SN zones (Meyer, Weaver, & Woosley 1995) and are constrained to reproduce the isotopic signatures of SiC X grains and to have C/O > 1. The equilibrium thermodynamic condensation calculations follow the scheme used by Lodders & Fegley (1995) for trace element abundances in SiC grains from carbon stars. The limitations of this approach, as well as consideration of mixing with nonhomogenized SN zones and the case C/O < 1, are discussed.

TABLE 1

B- AND SI-ISOTOPIC COMPOSITIONS AND B CONCENTRATIONS IN PRESOLAR SiC GRAINS FROM THE MURCHISON METEORITE

Grain	$\delta^{30}Si/^{28}Si$[a] (‰)	$^{11}B/^{10}B$	B/Si (10^{-5})	B/Si_{corr}[b] (10^{-5})
X100	-395 ± 21		0	0
X101	-386 ± 17		0.83	0.25
X102	-696 ± 15		0.28	0.08
X103	-525 ± 17		0.48	0.14
X104	-570 ± 14		1.5	0.45
X105	-240 ± 29		1.0	0.30
X106	-138 ± 15		1.3	0.39
X107	-520 ± 13		1.9	0.57
X108	-542 ± 14		1.9	0.57
X109	-362 ± 17		2.9	0.87
X110	-572 ± 28		5.0	1.5
SiC X total	$-140 \ldots -700$	3.46 ± 1.39	1.3[c]	0.39[c]
SiC Mainstream	$30 \ldots 170$	3.83 ± 0.42	2.1[c]	
Solar	0	4.04	2.1	

[a] $\delta^{30}Si/^{28}Si = [(^{30}Si/^{28}Si)/(^{30}Si/^{28}Si)_{\odot} - 1] \times 1000)$.
[b] $B/Si_{corr} = B/Si \times 0.30$. See text for details.
[c] Median value.

2. EXPERIMENTAL METHODS

Presolar SiC grains separated from the Murchison separate KJE (Amari, Lewis, & Anders 1994) were dispersed on a gold foil and studied by secondary ion mass spectrometry (SIMS). Eleven SiC type X grains were identified by ion imaging of the $^{30}Si/^{28}Si$ ratio, a method that allows quick recognition of rare types of presolar grains (Pungitore 1995; Nittler 1996). The SiC X grains are easily distinguished from the SiC mainstream grains (about 90% of all SiC grains) by their lower $^{30}Si/^{28}Si$ ratios. Subsequently, $^{11}B/^{10}B$, $^{30}Si/^{28}Si$, and B/Si ratios were measured in the X grains and, for comparison, in 18 SiC mainstream grains with the conventional SIMS analysis technique using the modified Cameca IMS3f ion microprobe at the Max-Planck-Institute for Chemistry at Mainz. The SiC grains were bombarded with O^- primary ions (≈ 100 pA, 17 keV) and low-energy positive secondary ions were measured at a mass resolution of ≈ 500. This is sufficient to resolve $^{30}Si^{+3}$ from $^{10}B^+$; all other potential isobaric interferences at masses 10, 11, and 30, such as ^9BeH, ^{10}BH, and ^{29}SiH, were shown to contribute by less than 1% to the respective ion intensities and are thus negligible. Total integration times on each SiC grain were 100–120 s for ^{10}B, 30–100 s for ^{11}B, 10 s for ^{28}Si, and 20 s for ^{30}Si. Corrections for spectrometer background (0.0012 counts s^{-1}) and contributions from the gold foil make up about 20% of the measured signal for ^{10}B in the presolar SiC grains. Boron-isotopic compositions were normalized to the respective values measured in NIST SRM 613 glass, Si-isotopic compositions to synthetic SiC. B/Si ratios were normalized to that measured in a 1:5 mixture (by mass) of BN (the expected boron compound in SiC; see below) and SiC. The secondary ion yields of boron (normalized to Si) in a number of silicate samples (NIST SRM 611, 613, and 615 glasses, and a Hawaiian basalt with 351, 32, 1.3, and 2.2 parts per million [ppm] B, respectively) were shown to be only about 25% lower than that in the BN-SiC mixture, indicating that matrix effects appear to be small. Comparable secondary ion yields for boron in silicate

samples have been reported from other ion microprobe studies (Hervig 1996; Chaussidon et al. 1997). We thus consider the measurement of B/Si ratios in SiC precise within several 10%.

3. RESULTS

The results of the SIMS analyses are summarized in Table 1 and Figure 1. The SiC X grains have $\delta^{30}Si/^{28}Si$ values between -140 and $-700‰$, within the range of the known X grains. Boron concentrations are generally low with typical B/Si ratios of 1×10^{-5} in the X grains, which is close to the solar ratio, and only slightly higher abundances in the mainstream grains. This corresponds to about 4 ppm or, respectively, 10^{-17} g boron in individual SiC grains. Huss, Hutcheon, & Wasserburg (1997) measured similar boron concentrations for six presolar SiC grains from the Orgueil meteorite. Owing to the low boron amounts, errors of $^{11}B/^{10}B$ ratios in single grains are very large, and only averages for X and mainstream grains are given in Table 1. Within analytical uncertainties, both X and mainstream grains have solar $^{11}B/^{10}B$ ratios.

4. DISCUSSION

4.1. *Boron-isotopic Ratio*

The average $^{11}B/^{10}B$ ratio measured in the X grains is clearly at odds with the expectations for dust from Type II SNe, which, averaged over the whole ejecta, is expected to be essential pure ^{11}B (WW95; cf. Figs. 2 and 3). Detailed hydrodynamic computer simulations of the mixing in Type II SN ejecta are still limited, and it is currently not possible to follow the mixing down to the microscopic scale. Nevertheless, ad hoc mixing calculations have shown that, in order to reproduce the isotopic signatures of SN grains,

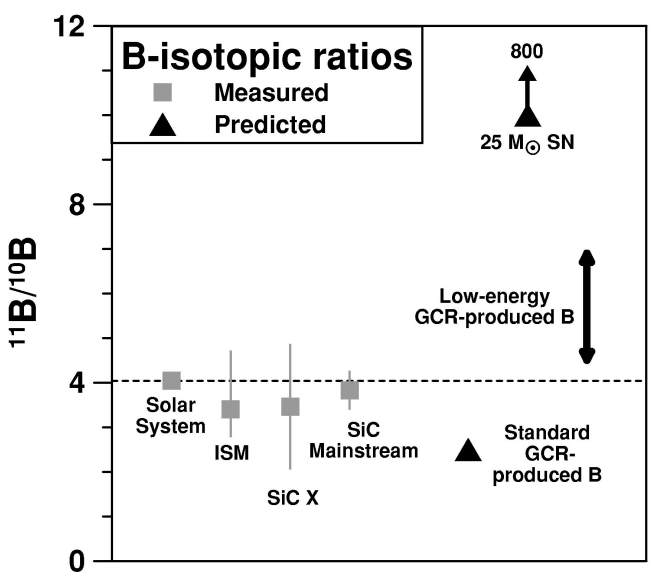

FIG. 2—Boron-isotopic ratios in the solar system, in the ISM (Federman et al. 1996), and in presolar SiC X and mainstream grains from the Murchison CM2 meteorite (this work). Predicted B-isotopic ratios from standard GCR spallation reactions (e.g., Meneguzzi et al. 1971), low-energy GCR spallation reactions (Meneguzzi et al. 1971; Cassé et al. 1995), and in the ejecta of a 25 $M_\odot$ Type II SN (WW95) are shown for comparison.

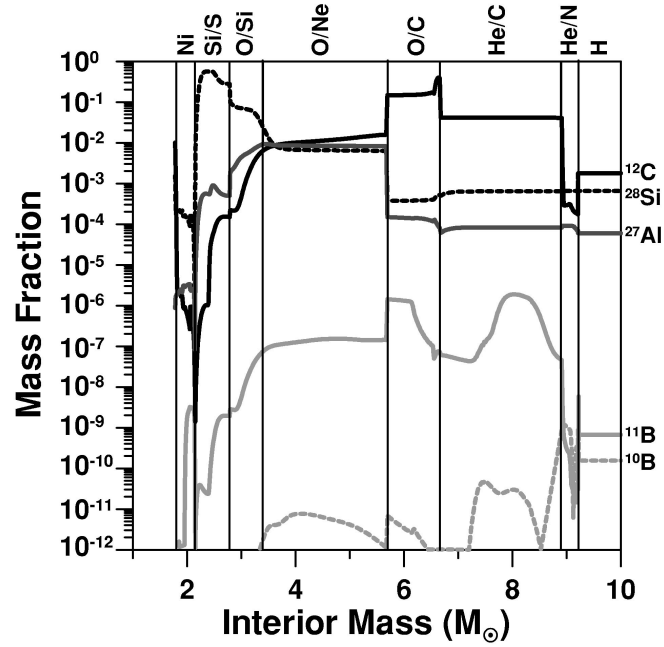

FIG. 3—Mass fractions of selected isotopes as a function of interior mass in a 25 $M_\odot$ Type II SN (WW95). The vertical lines divide the SN into eight distinct layers that are labeled according to the most abundant elements (cf. Meyer et al. 1995).

matter from only selected layers in the SN ejecta should be combined (Zinner et al. 1995; Hoppe et al. 1996, 2000; Nittler et al. 1996; Travaglio et al. 1999). All of these mixing calculations consider significant amounts of matter from the C-rich He/C zone (cf. Fig. 3). In this zone ^{11}B is most abundant. Any mixing that reproduces the C- and Si-isotopic signatures of the X grains reasonably well produces boron as almost pure ^{11}B. The separation of presolar SiC from meteorites relies on extensive chemical processing. Amari et al. (1994), e.g., used H_3BO_3 to remove fluorides, and a contamination with extraneous boron is possible. This possibility is also supported by the fact that the SiC mainstream grains show boron concentrations similar to those of the X grains although the winds of their parent stars are most likely low in boron (J. Lattanzio 2000, private communication; F. Herwig 2000, private communications). The close to solar $^{11}B/^{10}B$ ratio of X grains can be reconciled with the predictions for Type II SNe if the intrinsic SN boron makes up at most 30% of the measured boron. While the measured B-isotopic ratio is thus not very diagnostic with respect to boron production in Type II SNe, much more can be inferred from the boron concentrations in the SiC X grains (§ 4.2).

Although Type II SNe are the most likely sources of X grains, Type Ia SNe cannot be strictly excluded as an alternative source of SiC X grains (Clayton et al. 1997; Hoppe et al. 2000). Current models of Type Ia SNe (e.g., Clayton et al. 1997) do not indicate boron production. This reflects the fact that in a Type Ia SN explosion there are less neutrinos and target ^{12}C nuclei in comparison with a Type II SN explosion (B. Meyer 2000, private communication). Consequently, boron abundances are expected to be low in SiC grains from Type Ia SNe, and, provided that the SiC X grains are from Type Ia SNe, the boron seen in SiC X grains might be entirely of laboratory origin. A detailed discussion

of the boron data in view of Type Ia SN models is thus useless, and the following discussion will solely focus on boron in SiC dust from Type II SNe.

4.2. *Boron Abundances*

4.2.1. *Elemental Abundances in Type II SN Ejecta*

Mixtures considered for SiC condensation in Type II SN ejecta generally have element/Si ratios lower than solar for most elements (Fig. 4). Boron is a rare exception, typically strongly enriched relative to Si and solar. This is in contrast to the B/Si ratios in the X grains which, on average, are more than an order of magnitude lower than those in the SN mixtures considered here (Fig. 5). The situation is different for Al and Ti, whose elemental abundances relative to Si in 1 μm–sized X grains (Hoppe et al. 2000) are comparable to the ratios in the SN mixtures (Fig. 5). Large differences between trace elemental abundances in X grains and the SN mixtures are also evident for N, Mg, Ca, and Fe (Fig. 5). The SN mixtures used here are based on the data of Meyer et al. (1995) for a 25 $M_\odot$ Type II SN of solar metallicity, and we consider matter from the He/N, He/C, O/Si, and Si/S zones (for a definition of the zones see Fig. 3) in proportions that are able to cover the range of observed C-, Al-, and Si-isotopic compositions of X grains reasonably well. Similar mixing compositions are obtained if the 15 and 25 $M_\odot$ SN models of solar metallicity of WW95 are used. We will discuss condensation of B, N, Mg, Al, Ca, Ti, and Fe into SiC for five different SN mixtures (Fig. 4), and we shall discuss whether the low B/Si ratios seen in X grains can be explained by fractionation between boron and silicon during SiC condensation.

4.2.2. *Dust Formation in Type II SN Ejecta*

On the basis of the low amount of CO in Type II SN ejecta (Liu & Dalgarno 1995), Clayton, Liu, & Dalgarno (1999) argued that kinetic chemistry drives dust formation in Type II SN ejecta. The strong ^{56}Co radioactivity (half-life 77.3 days) produces abundant Compton electrons (Clayton & The 1991) and He^+ ions (Liu & Dalgarno 1995) in the ejecta, which can destroy the chemically very stable molecule CO (and many other less stable molecules). This leads to a supersaturation of carbon vapor and may allow formation of large graphite particles even if C/O < 1 (Clayton et al. 1999). While dust formation was observed in SN 1987A as early as 500 days after the explosion (Wooden 1997), no direct evidence for the formation of carbonaceous dust grains in Type II SNe has been obtained to date. Recently, Ebel & Grossman (2001) investigated the equilibrium condensation chemistry for an oxygen-rich SN shell where gaseous molecules (including CO) are absent. Only graphite may appear, but TiC and SiC are unstable. Thus, SiC formation at C/O < 1 is difficult to explain. Even if thermodynamic equilibrium would not apply in this scenario and SiC formation were kinetically driven, we emphasize that the problem remains why gaseous molecules, including the very stable CO molecule, are broken up by radiation but not the molecular clusters forming solids.

While kinetic chemistry might prevail during the first years after the explosion, equilibrium gas chemistry might play an important role later. The ^{56}Co decay rate scales with $\exp(-t/111$ days); i.e., it decreases by a factor of ≈ 3000 from day 100 to day 1000 after the explosion. Other radioactive nuclides such as ^{57}Co (half-life 272 days) have longer half-lives, but their abundances are lower than that of ^{56}Co. On the other hand, the density in the ejecta decreases with t^{-3} (homologous expansion), making grain

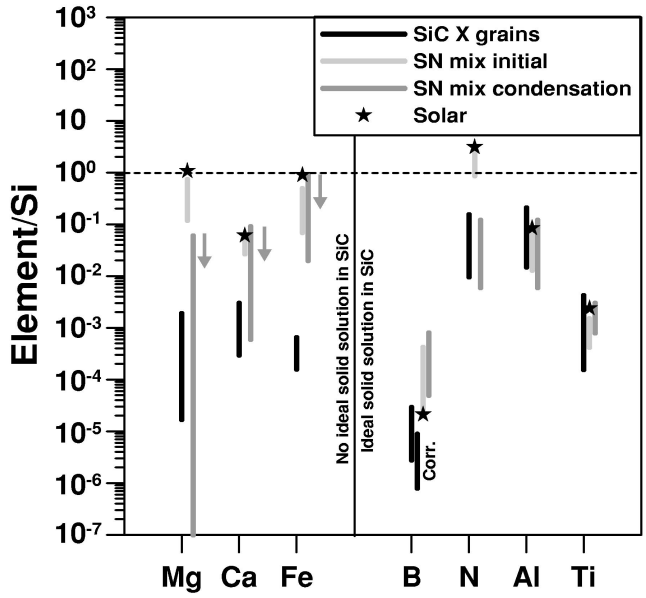

FIG. 5—Trace element abundances of N, Mg, Al, Ca, Ti, Fe (Hoppe et al. 2000), and B (this work) relative to Si in ≈ 1 μm–sized SiC X grains from the Murchison CM2 meteorite. For boron, both measured and corrected (for possible laboratory contamination) data are shown. The given ranges represent the data of about 90% of the grains. The solar ratios and predictions for SN shell mixing ("SN mix initial") and solid solution condensation into SiC ("SN mix condensation") are shown for comparison. Elements to the left of the vertical line do not form molecular compounds that favor ideal solid solutions into SiC, and calculated abundance ratios represent only upper limits (*arrows*). Elements to the right of the vertical line have molecular compounds that are expected to form ideal solid solutions with SiC.

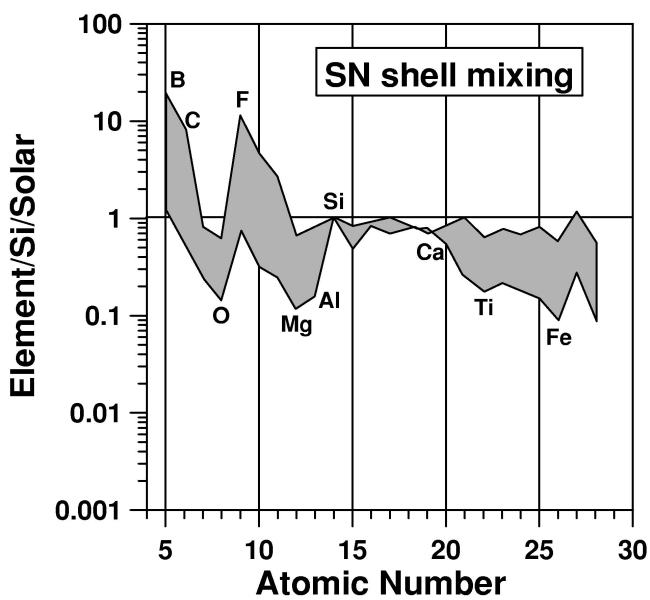

FIG. 4—Range of elemental compositions normalized to Si and solar in five SN mixtures (based on the data table of Meyer et al. 1995). See text for details.

growth more difficult at later times. However, clumpiness of the ejecta is predicted from hydrodynamic computer simulations (e.g., Ebisuzaki, Shigeyama, & Nomoto 1989; Fryxell, Müller, & Arnett 1991; Herant & Benz 1992; Herant & Woosley 1994) and has been observed in SN 1987A (see Wooden 1997). Consequently, the existence of isolated, dense C-rich regions in SN ejecta, even several years after the explosion, cannot be excluded, and condensation of small amounts of dust may take place under quasi-equilibrium conditions in such clumps. There is, indeed, observational evidence that the SiC X grains might have formed under quasi-equilibrium conditions. The SiC X grains have a grain-size distribution similar to that of the SiC mainstream grains (Hoppe et al. 2000). This suggests similar formation conditions for mainstream and type X SiC grains. However, in general, the size of carbonaceous dust depends on parameters such as gas density, C/O ratio, cooling rate, and residence time at the location of grain formation (see, e.g., Bernatowicz et al. 1996). The mainstream grains formed in the winds of carbon stars (see Hoppe & Ott 1997) and equilibrium gas chemistry have been successfully applied to explain the trace element abundances in these grains (Lodders & Fegley 1995).

4.2.3. *Condensation Calculations*

In the following we will calculate trace element abundances in SiC X grains assuming that they formed under equilibrium conditions. Computations were done with the CONDOR code described in detail elsewhere[5] (Fegley & Lodders 1994; Lodders & Fegley 1995). All SN mixtures considered here show C/O ratios above unity, and SiC condensation is expected under these conditions (see Table 2 and Figs. 4 and 5 for relative abundances of B, C, N, O, Mg, Al, Si, Ca, Ti, and Fe). The CONDOR code computes the equilibrium gas chemistry and condensation temperatures for all elements and their compounds. Condensation temperatures of major element compounds and trace element condensation in solid solution are done as described for trace element condensation into SiC around carbon stars (Lodders & Fegley 1995, 1997). Here results focus on the chemistry of B, C, N, Mg, Al, Si, Ca, Ti, and Fe. The total pressure in the calculation was kept constant at 10^{-7} bar. Both condensation temperatures and fractions of trace elements in solid solution with SiC typically scale with total pressure. Hence the relative condensation sequence as a function of temperature is relatively independent of the assumed pressure (Fig. 6).

About 100 boron gases (including ions) were considered in the calculations, and relevant boron solids include BN and B_4C (for B condensation at C/O < 1 see Lauretta & Lodders 1997). The major B-bearing gases in the selected SN mixes at 10^{-7} bar are B, BF, BHS, HBO, BS, BS_2, BO, and BFO in the temperature range of 1000–2000 K. These gas species are different than those in a solar composition gas or those in gas-giant planets (Fegley & Lodders 1994; Lauretta & Lodders 1997) because the C/O ratio is above unity here.

Condensation temperatures of pure substances are given in Table 2. Condensation of graphite takes place above 2000 K for all five abundance sets considered here. TiC, SiC, and other pure major condensates appear below 2000 K. CaS, AlN, BN, FeSi, and MgS are less refractory and condense at lower temperatures than SiC while more refractory TiC is condensed when SiC starts forming. Iron silicide (FeSi)—not iron carbide (Fe_3C) or metallic iron—is the first Fe-bearing condensate under reducing conditions (Lodders & Fegley 1999). However, an abundant condensate such as SiC can serve as a host phase for other (less abundant) condensates such as BN, AlN, or TiC, and solid solutions may form. The concentrations of elements other than C and

[5] See also http://solarsystem.wustl.edu for a comparison of the code to other results.

TABLE 2

CONDENSATION TEMPERATURES OF PURE SUBSTANCES AND 50% CONDENSATION TEMPERATURES FOR SOLID SOLUTION IN SiC AT $p = 10^{-7}$ BAR AND RELATIVE ABUNDANCES OF C, N, AND O[a] FOR FIVE DIFFERENT SN MIXTURES

C:N:O in Mixture	0.57:0.24:0.14	8.7:0.81:0.62	2.0:0.30:0.24	3.0:0.28:0.30	4.6:0.70:0.38
			T_{cond} (K) of Pure Substances		
C	2026	2189	2170	2186	2092
TiC	1619	1651	1665	1662	1590
SiC	1513	1498	1551	1540	1450
FeSi	1182	1228	1230	1230	1171
CaS	1179	1177	1209	1202	1134
AlN	1160	1194	1203	1197	1147
BN	1005	1148	1081	1107	1121
MgS	967	980	999	995	941
			$T_{cond,\ 50\%}$ (K) for Solid Solution in SiC		
SiC	1432	1365	1460	1448	1361
TiC	1513	1498	1551	1540	1450
Fe_3C	1220	1208	1252	1243	1167
CaS	1220	1211	1252	1244	1169
MgS	<1000	<1000	<1000	<1000	<1000
AlN	1229	1232	1264	1254	1191
BN	1482	1456	1509	1492	1412

[a] Normalized to Si and solar. In gas of solar composition C:N:O:Si = 10:3.1:24:1 (Anders & Grevesse 1989).

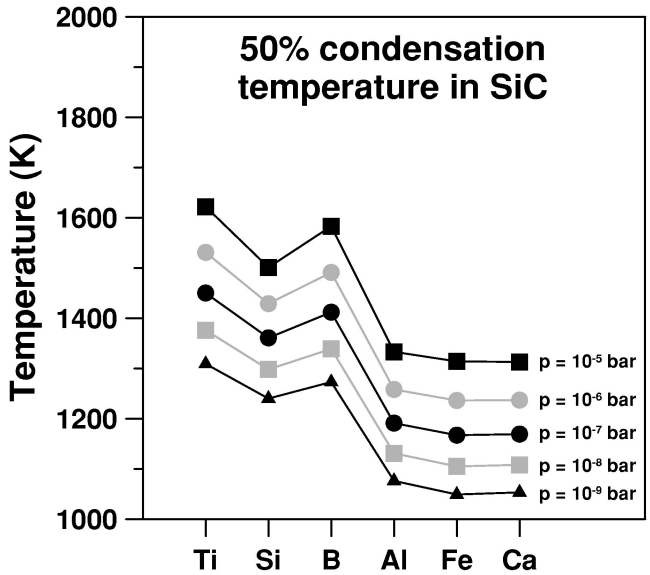

FIG. 6—50% condensation temperature as function of total pressure. Ideal solid solution with SiC is assumed for TiC, BN, AlN, Fe_3C, and CaS. The initial gas composition is that of SN mixture 5 (cf. Table 2). The relative condensation sequence does not depend on pressure.

Si in SiC grains depend on their ability to substitute Si and C in the SiC lattice, which is modeled by condensation into solid solution with SiC. The most stable pure condensates BN, MgS, AlN, CaS, and TiC, as well as Fe_3C, are the relevant molecular species considered for solid solution with SiC. The condensation temperatures for compounds in solid solution are different than their condensation temperatures as pure compounds. In Table 2 (*bottom*) we show the 50% condensation temperatures where half of the total abundance of an element is sequestered in SiC if solid solution occurs.

Solid solution occurs by substitution of Si and C atoms in the SiC lattice by other atoms. Upadhyaya (1996) summarizes the conditions determining the formation of solid solutions among carbides. In short, conditions favoring continuous solid solutions are (1) similar stoichiometric composition (e.g., same formulae of type A_xB_y), (2) similar crystal structures, (3) similar types of chemical bonds, and (4) small differences in atomic radii. AlN and BN fulfill all four criteria for solid solution formation with SiC. All three compounds are of stoichiometric type AB and form zincblende (cubic) and wurzite (hexagonal) crystal structures. The bonds are covalent and involve sp3 hybrids (Pierson 1996; Upadhyaya 1996). The covalent radii of Si and C atoms are 1.17 and 0.77 Å, and those for B, Al, and N are 0.83, 1.26, and 0.74 Å, respectively (Lodders & Fegley 1998). Thus, B and Al can easily substitute for Si and N for C. The substitution of C by N in SiC has been investigated by Hardeman (1963). The covalent radius of B is small enough that it can also substitute for C as found by Woodbury & Ludwig (1961). The properties of TiC do not match all criteria for solid solution but appear to be the next best case for it. It has the same stoichiometry (AB) as SiC but has a cubic NaCl-type crystal structure instead of the cubic zincblende type structure of cubic SiC. The bond type is characterized as interstitial, and the covalent radius of Ti (1.47 Å) is about 26% larger than that of Si. Iron carbide probably forms only limited solid solutions with SiC. Although the covalent radius of Fe (1.26 Å) is similar to that of Al and may substitute for Si in SiC, the stoichiometry of Fe_3C is different than that of SiC. The lattice of Fe_3C is distorted, and the bonding is described as intermediate (see Pierson 1996). The most stable compounds of Ca and Mg are MgS and CaS. Both compounds form NaCl-type crystal structures with ionic bonds, contrary to the covalent bonds in SiC. Sulfur (1.04 Å) is 35% larger than C and may replace C only to some extent. The similar radii of Si and S suggest that S could substitute for Si. Radii of Mg (1.38 Å) and Ca (1.7 Å) are 20% and 45% larger than that of Si. Thus, solid solution of MgS and CaS in SiC may be unfavorable.

BN and AlN are known to form solid solutions with SiC (e.g., Zangvil & Ruh 1985, 1988). In the absence of activity coefficient data for AlN and BN solid solutions in SiC, we assume ideal solid solution for modeling condensation into SiC. As seen below, any differences in the solid solution behavior of Al and B could be important. However, nothing is known about the ideality (i.e., heats of solution) of the BN-SiC or AlN-SiC solid solutions. The only information available about the heats of solution (or activity coefficients) is for metallic B and Al in SiC, which are about the same for both elements (Tajima & Kingery 1982). Therefore, we assume that the heat of solutions for AlN and BN in SiC are similar as well. In that case, any nonideal effect in the condensation of AlN and BN into SiC scales by the same factor from ideality. We also apply ideal solid solution to the condensation of TiC, MgS, CaS, or Fe_3C in SiC because essentially nothing is known about their solid solution behavior. However, the guidelines given above suggest that only minor fractions of MgS, CaS, and Fe_3C will actually be incorporated into SiC. This has to be considered in the discussion later.

The element/Si atomic ratios resulting from condensation in solid solutions with SiC are shown in Figure 5 for the different SN mixtures and temperatures below 1300 K. If all of a trace element and all Si is condensed into SiC, the element/Si abundances plot at the lines "SN mix initial" shown in Figure 5. However, at high temperatures, only a small amount of Si is condensed in SiC, and the fraction of Si in SiC increases with decreasing temperature. Similarly, the amount of trace elements in solid solution with SiC increases as temperature drops. Thus, the element/Si ratio depends on the amounts of trace element and Si condensed. These ratios were calculated in 100 K temperature increments beginning near the temperatures where SiC starts condensing in the different mixtures. Only about half of all Si condenses as SiC. The remaining Si condenses either as forsterite (Mg_2SiO_4) or FeSi at lower temperatures (see Lodders & Fegley 1995, 1997, 1999 for a detailed discussion of this). This is why the maximum element/Si ratios for the trace elements shown in Figure 5 (except Mg) plot about 2 times higher than the maximum values in the mixtures once all of a trace element is condensed at low temperatures.

The calculated element/Si patterns in Figure 5 ("SN mix condensation") are compared to the measured element/Si ratios in the SiC grains in order to see if there is a temperature where they match. Ratios calculated below 1300 K coincide with the observed abundance ratios for N, Al, and Ti. This implies that complete solid solution formation of AlN and TiC with SiC occurred in the samples. On the other hand, at temperatures where the predicted and

observed Al/Si and Ti/Si ratios match, the corresponding ratios of B/Si and Fe/Si do not overlap at all. The predicted ranges for Mg/Si and Ca/Si extend to higher values than those observed in the grains (Fig. 5). This mismatch is present for all examined SN shell mixtures. For Mg, Ca, and Fe such disparity was also found for mainstream SiC grains from carbon stars (see Lodders & Fegley 1995). Above we discussed that ideal solid solution of MgS, CaS, and Fe_3C in SiC may not apply. Moreover, Mg, Ca, and Fe are among the more abundant elements, and MgS, CaS, and FeSi condensation temperatures for pure compounds are close to those where some MgS, CaS, and Fe_3C might be in solid solution. Formation of such pure condensates may compete with solid solution formation.

The agreement of calculated and observed Al/Si ratios (Fig. 5) suggests that fractional condensation occurred to low enough temperatures for complete AlN incorporation into SiC. The calculated B/Si ratios for all mixtures are typically much higher (by more than an order of magnitude on average) than observed in the grains. The calculated B/Si abundances in solid solution are always closer to the B/Si ratio of the mixtures than the respective Al/Si ratios until temperatures low enough that Al is fully incorporated as AlN. At the temperatures where calculated and observed Al/Si ratios coincide, all Al is condensed as AlN in SiC, and then B is expected to be fully condensed too. Thus, the B/Al ratio (as well as B/Si and Al/Si ratios; see Fig. 5) in the SiC grains reflects the B/Al ratio in the source region of the grains. Consequently, the predicted B abundances in regions of SN ejecta from which the SiC X grains formed are too high, and possible implications will be discussed in § 5.

4.2.4. *The Role of Nitrogen*

Nitrogen plays a key role in the condensation chemistry of B and Al. Aluminum and N are the two most abundant trace elements in the SiC X grains. According to our calculations, all Al and most of the condensable N is expected to have condensed as AlN into SiC, and one would expect to find an atomic ratio of Al/N ≈ 1 in the grains. The average Al/N ratio reported for 1 μm–sized X grains is 1.4 (but note that there are no simultaneous Al and N determinations from the same grains; Hoppe et al. 2000), while that for large (2–10 μm) X grains is 2.5 (L. Nittler et al. 2000, in preparation), indicating a nonstoichiometric Al/N ratio. However, while the measured trace element abundances are generally precise within 20%–30%, this is clearly not the case for nitrogen. The currently used nitrogen calibration is precise within only a factor of 2–3 (Hoppe et al. 1995). Consequently, the Al and N data are compatible with the assumption that major fractions of Al and N were incorporated as AlN into the SiC X grains. Some large X grains have Al/N ratios distinctly higher than those of most X grains (L. Nittler et al. 2000, in preparation). In these cases a contamination with Al-rich oxide grains cannot be excluded. This possibility is supported by the comparatively lower ^{26}Al/^{27}Al ratios in X grains with high Al/N.

5. SUMMARY AND CONCLUSIONS

Boron, N, Al, and Ti condense as BN, AlN, and TiC that form ideal solid solutions with SiC. Equilibrium condensation calculations for Type II SN ejecta show good agreement between predicted and observed abundances in SiC X grains for N, Al, and Ti, but not for B. The measured B/Al ratios are lower than those predicted from SN mixtures. Given the similarity of the B and Al condensation chemistry, the difference between measured and predicted B/Al ratios in SiC X grains must be considered a significant problem provided that (1) X grains are from Type II SNe (and not from Type Ia SNe), (2) the mixing in SN ejecta involves isotopically homogenized SN zones, and (3) condensation occurred from a gas with C/O > 1. While it is not apparent how nonequilibrium chemistry could solve the discrepancy between measured and predicted B/Al ratios, consideration of isotopically nonhomogenized SN zones and SN mixtures with C/O < 1 requires a closer inspection (see below). We also note that the B/Al ratio problem does not result from the correction made for possible extraneous boron contamination. Without this correction, the difference between total measured and predicted B/Al ratios is still larger than a factor of 10. Without this correction, however, the observed ^{11}B/^{10}B ratios in the X grains are clearly at odds with the expectations for boron from Type II SNe.

Possible solutions for the problem of higher predicted than measured B/Al ratios include the following:

1. The boron production from neutrino reactions with carbon in Type II SNe is lower than predicted. This, however, leaves the solar boron abundance and ^{11}B/^{10}B ratio unexplained. The production of ^{11}B in Type II SNe depends on the temperature of the τ and μ neutrinos (WW95). Our boron data suggest a lower neutrino temperature T_ν than the 8 MeV used by WW95. For $T_\nu = 6$ MeV (probably more reasonable; S. Woosley 2000, private communication) the production of ^{11}B is about a factor of 2 lower. Reduction of the production of ^{11}B by another factor of 2 appears possible because of uncertainties in the relevant nuclear cross sections (S. Woosley 2000, private communication).

2. Our mixing calculations assume homogeneous isotopic abundances in the different SN zones. Many isotopes are indeed homogeneously distributed over a given zone because convection during pre-SN evolution tends to mix material within a given zone (Meyer et al. 1995). There are, however, exceptions to this. Among them are ^{11}B and ^{15}N in the He/C zone (WW95). Rayleigh-Taylor instabilities develop at layer boundaries during the explosion, and only sublayers of a given SN zone might be involved in the mixing. If we, for example, assume that only the inner portion of the He/C zone contributed matter to the SiC condensation site in the ejecta, then the B/Al ratio problem could be considerably relaxed. There the B/Al ratio is about an order of magnitude lower than the average over the entire He/C zone (Fig. 3). Similarly, preferential formation of nitrides at the bottom of the He/C zone was invoked by Travaglio et al. (1999) and Hoppe et al. (2000) in order to account for the N-isotopic signatures seen in low-density graphite and SiC X grains.

3. Consideration of mixtures with C/O < 1 because Al is abundant in the O-rich regions of SNe (WW95; see Fig. 3). As first shown by Gilman (1969), equilibrium condensation of SiC can occur from only an otherwise solar composition gas that has C/O > 1. In Type II SNe, however, carbonaceous grains may condense even if C/O < 1 (Clayton et al. 1999). In order to account for the observed B/Al (and B/Si and Al/Si) ratios in X grains, the SN mixtures must have

C/O < 0.1. Whether SiC actually forms under these conditions is doubtful (see above and Ebel & Grossman 2001), and how Al and B condensation into SiC is affected has yet to be explored. Moreover, this solution introduces new problems since $^{26}Al/^{27}Al$ is comparatively low in the O-rich zones of Type II SNe (WW95), contrary to the X grain data.

Assuming that SiC X grains are from Type II SNe, solutions 1 and 2 are preferred because solution 3 introduces new problems. A combination of solutions 1 and 2 can reduce the expected B/Si and B/Al ratios at the SiC condensation site in the ejecta of a Type II SN by factors of $\approx$ 20–40, and a fairly good match with the X grain data could be achieved.

We thank Larry Nittler for his critical and constructive review that helped to improve this manuscript and for making unpublished X grain data available to us. We also wish to thank Stan Woosley for the detailed data on 15 and 25 $M_{\odot}$ SN models and Bruce Fegley for helpful comments. This work was supported by NASA grants NAG5-4323 (K. L.; NASA Origins Program) and NAG5-4297 (R. L.).

REFERENCES

Amari, S., Hoppe, P., Zinner, E., & Lewis, R. S. 1992, ApJ, 394, L43
Amari, S., Lewis, R. S., & Anders, E. 1994, Geochim. Cosmochim. Acta, 58, 459
Anders, E., & Grevesse, N. 1989, Geochim. Cosmochim. Acta, 53, 197
Anders, E., & Zinner, E. 1993, Meteoritics, 28, 490
Bernatowicz, T. J., Cowsik, R., Gibbons, P. C., Lodders, K., Fegley, B., Jr., Amari, S., & Lewis, R. S. 1996, ApJ, 472, 760
Bloemen, H., et al. 1994, A&A, 281, L5
———. 1999, ApJ, 521, L137
Cassé, M., Lehoucq, R., & Vangioni-Flam, E. 1995, Nature, 373, 318
Chaussidon, M., & Robert, F. 1995, Nature, 374, 337
Chaussidon, M., Robert, F., Mangin, D., Hanon, P., & Rose, E. F. 1997, Geostandard Newsletter, 21, 7
Clayton, D. D. 1994, Nature, 368, 222
Clayton, D. D., Arnett, W. D., Kane, J., & Meyer, B. S. 1997, ApJ, 486, 824
Clayton, D. D., Liu, W., & Dalgarno, A. 1999, Science, 283, 1290
Clayton, D. D., & The, L.-S. 1991, ApJ, 375, 221
Ebel, D. S., & Grossman, L. 2001, Geochim. Cosmochim. Acta, 65, 469
Ebisuzaki, T., Shigeyama, T., & Nomoto, K. 1989, ApJ, 344, L65
Federman, S. R., Lambert, D. L., Cardelli, J. A., & Sheffer, Y. 1996, Nature, 381, 764
Fegley, B., & Lodders, K. 1994, Icarus, 110, 117
Fryxell, B., Müller, E., & Arnett, D. 1991, ApJ, 367, 619
Gilman, R. C. 1969, ApJ, 155, L185
Hardeman, G. E. G. 1963, J. Phys. Chem., 24, 1223
Herant, M., & Benz, W. 1992, ApJ, 387, 294
Herant, M., & Woosley, S. E. 1994, ApJ, 425, 814
Hervig, R. L. 1996, in Reviews in Mineralogy, Vol. 33, Boron: Mineralogy, Petrology and Geochemistry, ed. E. S. Grew & L. M. Anovitz (Washington, D.C.: Mineralogical Society of America), 789
Hoppe, P., Amari, S., Zinner, E., & Lewis, R. S. 1995, Geochim. Cosmochim. Acta, 59, 4029
Hoppe, P., & Ott, U. 1997, in AIP Conf. Proc. 402, Astrophysical Implications of the Laboratory Study of Presolar Materials, ed. T. J. Bernatowicz & E. Zinner (New York: AIP), 27
Hoppe, P., Strebel, R., Eberhardt, P., Amari, S., & Lewis, R. S. 1996, Science, 272, 1314
———. 2000, Meteoritics Planet. Sci., 35, 1157
Hoppe, P., & Zinner, E. 2000, J. Geophys. Res., 105, 10371
Huss, G. R., Hutcheon, I. D., & Wasserburg, G. J. 1997, Geochim. Cosmochim. Acta, 61, 5117
Lauretta, D. S., & Lodders, K. 1997, Earth Planet. Sci. Lett., 146, 315
Liu, W., & Dalgarno, A. 1995, ApJ, 454, 472
Lodders, K., & Fegley, B. J. 1995, Meteoritics, 30, 661
Lodders, K., & Fegley, B., Jr. 1997, in AIP Conf. Proc. 402, Astrophysical Implications of the Laboratory Study of Presolar Materials, ed. T. J. Bernatowicz & E. Zinner (New York: AIP), 391
Lodders, K., & Fegley, B. 1998, The Planetary Scientist's Companion (New York: Oxford Univ. Press)
———. 1999, in IAU Symp. 191, Asymptotic Giant Branch Stars, ed. T. LeBertre, A. Lebre, & C. Waelkens (San Francisco: ASP), 279
Meneguzzi, M., Audouze, J., & Reeves, H. 1971, A&A, 15, 337
Meyer, B. S., Weaver, T. A., & Woosley, S. E. 1995, Meteoritics, 30, 325
Nittler, L. R. 1996, Ph.D. thesis, Washington Univ.
Nittler, L. R., Amari, S., Zinner, E., Woosley, S. E., & Lewis, R. S. 1996, ApJ, 462, L31
Nittler, L. R., et al. 1995, ApJ, 453, L25
Olive, K. A., Prantzos, N., Scully, S., & Vangioni-Flam, E. 1994, ApJ, 424, 666
Ott, U. 1993, Nature, 364, 25
Pierson, H. O. 1996, Handbook of Refractory Carbides and Nitrides (Westwood: Noyes)
Pungitore, B. 1995, M.S. thesis, Univ. Bern
Ramaty, R., Kozlovsky, B., & Lingenfelter, R. E. 1996, ApJ, 456, 525
Tajima, Y., & Kingery, W. D. 1982, J. Am. Ceram. Soc., 65, 27
Timmes, F. X., Woosley, S. E., & Weaver, T. A. 1995, ApJS, 98, 617
Travaglio, C., Gallino, R., Amari, S., Zinner, E., Woosley, S., & Lewis, R. S. 1999, ApJ, 510, 325
Upadhyaya, G. S. 1996, Nature and Properties of Refractory Carbides (Commack: Nova Sci. Pub.)
Woodbury, H. H., & Ludwig, G. W. 1961, Phys. Rev., 124, 1083
Wooden, D. H. 1997, in AIP Conf. Proc. 402, Astrophysical Implications of the Laboratory Study of Presolar Materials, ed. T. J. Bernatowicz & E. Zinner (New York: AIP), 317
Woosley, S. E., & Weaver, T. A. 1995, ApJS, 101, 181
Yoshida, T., Emori, H., & Nakazawa, K. 2000, Earth Planets Space, 52, 203
Zangvil, A., & Ruh, R. 1985, Mater. Sci. Eng., 71, 159
———. 1988, J. Am. Ceram. Soc., 71, 884
Zinner, E. 1998, Annu. Rev. Earth Planet. Sci., 26, 147
Zinner, E., Amari, S., Travaglio, C., Gallino, R., Busso, M., & Woosley, S. 1995, Lunar Planet. Sci., 26, 1561